STATISTICAL SCATTER OF THE ENERGY LOSS OF LOW-TEMPERATURE CHARGED PARTICLES

V. S. KESSEL'MAN

Submitted March 4, 1970

Zh. Eksp. Teor. Fiz. 59, 834–844 (September, 1970)

We determine the distribution function of the energy loss of low-energy particles passing through a "thin layer of matter" (i.e., when the loss is smaller than the initial particle energy) with allowance for the multiple scattering effect.

A charged low-energy particle (ion) passing through a layer of matter loses energy as a result of elastic and inelastic ("electronic") collisions with the atoms of this matter. Owing to fluctuations, the particle energy loss is not constant, and therefore ions having the same initial energy will emerge from a certain layer of uniform thickness with noticeably different energies. The fluctuations in the elastic collisions are connected with the fact that certain collisions occur with a transfer of energy much larger than the average value. In the case of separate inelastic collision, the ions lose in the main only a small fraction of their energy, and the fluctuations of the energy loss are due in this case to fluctuations in the number of the inelastic collisions. In addition, a definite contribution to the total statistical scatter of the energy loss is made by fluctuations connected with the effect of multiple scattering, i.e., with the differences between the true paths of the ion in the medium for different ions having identical initial energies.

A theoretical analysis of the statistical scatter of the energy loss was made in a number of papers (see the paper of Starodubtsev and Romanov[1], where references to work by others can be found), but the results obtained there pertain to the region of large initial ion energies, namely to the region in which the average energy loss of the charge particle is determined by the Bethe-Bloch formula.

In this paper we consider the energy loss of low-energy ions. By low-energy ions we mean ions whose energy is such that the theory of Lindhard and co-workers (henceforth denoted LSS) is valid[2]. As is well known, the LSS theory is valid for ions whose velocity is $v \lesssim v_1 = Z_1^{2/3} v_0$ (Z_1—atomic number of particles, v_0—electron velocity at the first Bohr orbit of the hydrogen atom, equal to 2.2×10^8 cm/sec) or $E \lesssim E_1 = 25 Z A_1$ (keV).

In the LSS theory, the energy loss in elastic and inelastic collisions is regarded as a continuous and uncorrelated process, and the energy E and the range R of the ion are expressed in the dimensionless variables ϵ and ρ:

$$\varepsilon = \frac{a_{TF} A_2}{Z_1 Z_2 e^2 (A_1 + A_2)} E, \quad \rho = N \pi a_{TF}^2 \gamma R. \tag{1}$$

where A_1, A_2, $z_1 e$, and $z_2 e$ are respectively the mass numbers and the charges of the ion and of the atom of the medium producing the deceleration, N is the density of the atoms of the medium, $\gamma = 4A_1A_2(A_1 + A_2)^{-2}$,

$$a_{TF} = 0.8853(\hbar^2/me^2)(Z_1^{2/3} + Z_2^{2/3})^{-1/2} = 0.468(Z_1^{2/3} + Z_2^{2/3})^{-1/2} (\text{Å}) \tag{2}$$

is the Thomas-Fermi screening radius in the form proposed by Lindhard for the case of the interaction of two atoms[3].

We denote the unknown distribution function by $f(r, \Delta)$: it represents the probability that an ion with a given initial energy ϵ, passing through a layer of matter r, loses a fraction of energy lying between Δ and $\Delta + d\Delta$ (ϵ, r, and Δ are written in terms of the dimensionless variables of the LSS theory). The layer of matter r is assumed to be so small, that the energy lost in it is small compared with the initial ion energy. The kinetic equation for the distribution function is

$$\frac{\partial f}{\partial r} = \frac{1}{\gamma} \int_0^{\gamma\varepsilon} \omega(u) [f(r, \Delta - u) - f(r, \Delta)] du - \left(\frac{d\varepsilon}{dr}\right)_e \frac{\partial f}{\partial \Delta}. \tag{3}$$

In (3), $(d\epsilon/dr)_e$ is the slowing-down ability for inelastic collisions:

$$\left(\frac{d\varepsilon}{dr}\right)_e = S_e N = K\varepsilon^{1/2}, \quad K = \zeta_e \left[\frac{0.0793 Z_1^{1/2} Z_2^{1/2} (A_1 + A_2)^{3/2}}{(Z_1^{2/3} + Z_2^{2/3})^{3/4} A_1^{3/2} A_2^{1/2}}\right]. \tag{4}$$

The constant ζ_e in (4) is of the order of $Z_1^{1/6}$. It is shown that oscillations occur in the value of K, owing to the shell structure of the atom[4]. The function $\omega(u)$ is the probability (per unit path length) of the energy loss in elastic collisions:

$$\omega(u) = \frac{\varepsilon}{\gamma} f\left[\left(\frac{\varepsilon u}{\gamma}\right)^{1/2}\right] \frac{1}{2} \left(\frac{\varepsilon u}{\gamma}\right)^{-3/2}. \tag{5}$$

The scattering function $f[(\epsilon u/\gamma)^{1/2}] = f(t^{1/2})$ was calculated in the LSS theory by numerical methods on the basis of the Thomas-Fermi statistical model of the atom, and its plot is shown in Fig. 1. We note that the quantity $t^{1/2} = \epsilon \sin(\theta/2)$ (θ is the scattering angle in the c.m.s.) determines the depth of penetration of the ion into the electron shell of the atom. In the case of a power-law potential in the form $V(r) = z_1 z_2 e^2 k_s a_s^{s-1} r^{-s}$, the function $f(t^{1/2})$ can be expressed as follows:[1)]

$$f(t^{1/2}) = f_s(t^{1/2}) = \lambda_s t^{1/2 - 1/s}, \quad 1 < s < 4, \tag{6}$$

where $\lambda_s = (2/s)(k_s \gamma_s/2)^{2/s}$ (k_s is a constant close to unity, and the values of γ_s are given in[3]). For s = 2 we have

$$f_2(t^{1/2}) = \lambda_2 = k_2 \pi / 8 = 0{,}327.$$

To solve Eq. (3) we use the Fourier transformation

[1)] For a power-law potential, the differential cross section for energy transfer in elastic collisions can be obtained on the basis of the quasiclassical approximation, i.e., by a method different from that used in the LSS theory.

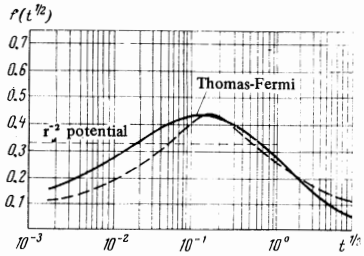

FIG. 1. Plots of the functions $f(t^{1/2})$ and $f_S(t^{1/2})$ ($\lambda_3 = 0.86$, $\lambda_{3/2} = 0.25$).

with respect to the independent variable Δ. Multiplying both sides of (3) by $e^{-i\lambda\Delta}$, integrating with respect to Δ from $-\infty$ to $+\infty$, and using the theorem concerning the Fourier transformation of the convolution of two functions, we obtain

$$\frac{\partial}{\partial r}\varphi(r,\lambda)=\frac{1}{\gamma}\varphi(r,\lambda)\int_0^{\gamma\varepsilon}(e^{-i\lambda u}-1)\,\omega(u)\,du-i\lambda\left(\frac{\partial\varepsilon}{\partial r}\right)_e\varphi(r,\lambda), \quad (7)$$

$$\varphi(r,\lambda)=\int_{-\infty}^{\infty}f(r,\Delta)\,e^{-i\lambda\Delta}d\Delta. \quad (7')$$

Integrating (7) with allowance for the fact that at $r = 0$ we have $f(0, \Delta) = \delta(\Delta)$ and then using the inverse Fourier transformation, we obtain the following expression for the distribution function:

$$f(r,\Delta)=\frac{1}{2\pi}\int_{-\infty}^{\infty}\exp\left\{i\lambda\left[\Delta-r\left(\frac{d\varepsilon}{dr}\right)_e\right]+\frac{r}{\gamma}\int_0^{\gamma\varepsilon}\omega(u)\,(e^{-i\lambda u}-1)\,du\right\}d\lambda. \quad (8)$$

To be able to find the form of the function $f(r, \Delta)$ it is necessary to calculate the integral in the exponential of (8). We present below a calculation of this integral under different approximations of $\omega(u)$ and of the function $f(r, \Delta)$ and indicate the limits of applicability of the corresponding formulas.

1. CALCULATION OF THE FUNCTION f(r, Δ)

We assume that in the second integral of (8) the upper integration limit is equal to infinity. This can be done, since $\omega(u)$ decreases rapidly at large values of u, and $\omega(u) = 0$ when $u > u_{max}$. We then use different approximations of $\omega(u)$.

A. Power-law Potential (s = 2)

The case $s = 2$, as follows from (6′) corresponds to the independence of $f_S(t^{1/2})$ of t. Such an approximation of the scattering function is valid in the region of values of the energy parameter $\epsilon \lesssim 1$. It should be noted here that in the case of not very light ions at such values of ϵ it is possible to neglect in (8) the term connected with the inelastic loss. For $s = 2$ we have

$$\omega(u)=\frac{A_2}{u^{3/2}},\quad A_2=\frac{\lambda_2}{2}\left(\frac{\gamma}{\varepsilon}\right)^{1/2}. \quad (9)$$

When $\omega(u)$ is expressed by formula (9), it is possible to calculate analytically the integral in the exponential of (8). Substituting (9) in (8) we obtain ultimately

$$f(r,\Delta)=\frac{1}{\beta^2}\varphi(\xi), \quad (10)$$

$$\varphi(\xi)=\frac{1}{4\sqrt{\pi}}\frac{1}{\xi^{3/2}}e^{-1/4\xi},\quad \xi=\frac{\Delta}{2\beta^2},\quad \beta=\frac{r}{\gamma}\sqrt{2\pi A_2}. \quad (10')$$

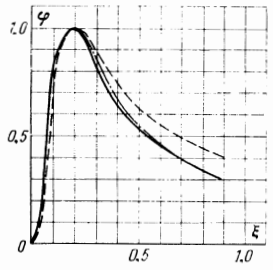

FIG. 2. Plots of the function $\varphi(\xi)$: solid curve—without allowance for multiple scattering, dashed and dash-dot curves—with allowance for multiple scattering.

Thus, the function $f(r, \Delta)$ of two variables is presented in the form of the product of $1/\beta^2$ by the universal function $\varphi(\xi)$ of the dimensionless variable ξ. A plot of the function $\varphi(\xi)$ is shown in Fig. 2 (solid line). When $\xi \approx 0.17$ this function has a maximum, and the mean value corresponds to $\langle\xi\rangle = 0.50$. Thus, the average and most probable values of the energy loss do not coincide and the $\varphi(\xi)$ curve has a right-hand asymmetry. The part of the curve on Fig. 2 to the left of the maximum ($\Delta < \Delta_0 = 0.17 \times 2\beta^2$, i.e., the energy loss is smaller than the most probable value) decreases very rapidly, and to the right of the maximum ($\Delta > \Delta_0$) it decreases much more slowly, approximately like $\xi^{-3/2}$. The median of the considered distribution (i.e., the line parallel to the ordinate axis and dividing the area of this curve into two equal parts) passes through a value of ξ approximately equal to 0.925.

B. General Case. Power-law Potential (s = 3 and s = 3/2)

In order to calculate the integral in the exponential of the integrand, let us assume that the only values of λ that matter in this integral are those for which the following conditions are satisfied:

$$\lambda u_1 \ll 1,\quad \lambda u_{max} \gg 1. \quad (11)$$

Here u_1 corresponds to the maximum of the function $f(t^{1/2})$ ($t^{1/2}_{max} \approx 0.15$), and $u_{max} = \gamma\epsilon$. The limitations which the assumption (11) imposes on the region of applicability of the results will be considered below.

Let us break up the integral with respect to du into two integrals with limits respectively from zero to u_1 and from u_1 to infinity. In the first region of the values of u, we approximate the function $f(t^{1/2})$ by the expression

$$f(t^{1/2})=f_3(t^{1/2}),\quad \omega(u)=\frac{A_3}{u^{1/2}},\quad A_3=\frac{\lambda_3}{2}\left(\frac{\gamma}{\varepsilon}\right)^{1/2} \quad (12)$$

and in the second region

$$f(t^{1/2})=f_{3/2}(t^{1/2}),\quad \omega(u)=\frac{A_{3/2}}{u^{1/2}},\quad A_{3/2}=\frac{\lambda_{3/2}}{2}\left(\frac{\gamma}{\varepsilon}\right)^{3/2}. \quad (13)$$

The approximating curves are shown dashed in Fig. 1. In the region $0 < u \leq u_1$, the $f_3(t^{1/2})$ curve lies somewhat lower than the plot of the function $f(t^{1/2})$. However, as will be shown below, the resultant error is not appreciable, and at very small values of t ($t^{1/2} \lesssim 0.01$) (corresponding to large approach distances between the atoms, and consequently to the case when the properties of the system of the interacting atoms are governed principally by the external electrons) this approximation agrees better with the real picture of the inter-

atomic interaction than the function[2] $f(t^{1/2})$ of Fig. 1.

In the region $u > u_1$ the $f_{3/2}(t^{1/2})$ curve with $t^{1/2} > 2$ lies above the plot of $f(t^{1/2})$. In this region values of t, the energy loss in the inelastic collisions grow in importance with increasing ϵ, and therefore the error due to such an approximation decreases with increasing contribution of the inelastic energy loss to the decelerating ability.

Using (12), (13), and the conditions (11) we obtain, leaving out the intermediate steps, the following expression for the integral in the exponential of (8):

$$\frac{r}{\gamma}\int_0^\infty \omega(u)\,(e^{-i\lambda u}-1)\,du = i[\lambda b + c\lambda^{2/3} - a] + \frac{\sqrt{3}}{3}c\lambda^{2/3} - \frac{2}{\sqrt{3}}a, \quad (14)$$

where

$$b = \frac{3}{2}\frac{r}{\gamma}A_3 u_1^{2/3}, \quad c = \frac{\sqrt{3}}{2}\Gamma\left(-\frac{2}{3}\right)\frac{r}{\gamma}A^{1/2}, \quad a = \frac{3\sqrt{3}}{4}\frac{r}{\gamma}A^{1/2}u_1^{-2/3}. \quad (15)$$

Substituting (14) in (8), we obtain an integral for the calculation of $f(r, \Delta)$:

$$f(r,\Delta) = \frac{e^{-2a/\sqrt{3}}}{\sqrt{2\pi}}\int_{-\infty}^{\infty}\exp\left[i(\eta\lambda - |c|\lambda^{2/3} - a) - \frac{\sqrt{3}}{3}|c|\lambda^{2/3}\right]d\lambda, \quad (16)$$

where

$$\eta = \Delta - r(d\varepsilon/dr)_e - b. \quad (16')$$

Introducing a new integration variable $y = |c|^{3/2}\lambda$, we obtain for the distribution function the following integral representations:

$$f(r,\Delta) = \frac{1}{\beta_1}\varphi(\tau), \quad (17)$$

where

$$\varphi(\tau) = \frac{1}{\pi}\int_{-\infty}^{\infty} e^{-y^{2/3}}\cos(\tau y - \sqrt{3}\,y^{2/3} - a)\,dy, \quad (18)$$

$$\tau = \eta|c|^{-3/2}, \quad \beta_1^{-1} = e^{-2a/\sqrt{3}}|c|^{-3/2}. \quad (19)$$

Thus, just as in the case of subsection A, the function $f(r, \Delta)$ turns out to be expressed in terms of the universal function $\varphi(\tau)$ of the dimensionless variable τ. The function $\varphi(\tau)$ is even and depends on a single parameter a, with respect to which it is periodic with a period 2π. This function was calculated with a computer with the parameter a taken on the values 0.5, 1.0, 10, 50, and 100, and its plots are shown in Figs. 3 and 4. The function $\varphi(\tau)$ to the left of the maximum ($\tau < \tau_{max}$) decreases more rapidly, and to the right of the maximum ($\tau > \tau_{max}$) it decreases more slowly with increasing τ. The value of Δ_0 corresponding to the most probable energy loss is given by the formula

$$\Delta_0 = r\left(\frac{d\varepsilon}{dr}\right) + b + |c|^{3/2}\tau_{max}, \quad (20)$$

where τ_{max} is the value of τ at which $\varphi(\tau)$ has a maximum.

Let us determine the region of applicability of the results. Obviously, in the integral (18) the principal role is played by the values $y \sim 1$. Taking this into account, we find that the assumptions (11) reduce to the conditions

$$(\gamma\varepsilon^{4/3}/r\lambda^{2/3}) \gg 1, \quad (0.1\gamma/r\lambda^{2/3}) \ll 1. \quad (21)$$

[2] Detailed tables of the function $f(t^{1/2})$ with allowance for the Fermi-Amaldi correction will be published later.

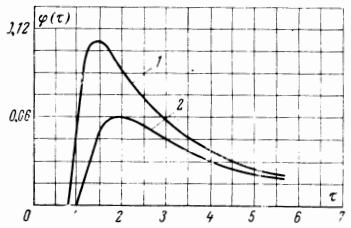

FIG. 3. The function $\varphi(\tau)$ for different values of the parameters a: 1–a - 0.5; 2–a - 1.0.

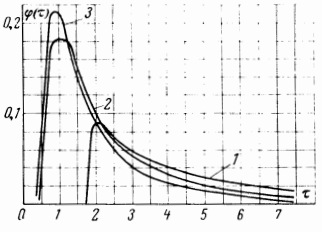

FIG. 4. The function $\varphi(\tau)$ for the values of the parameter a: 1–a = 10, 2–a = 50, 3–a = 100.

The inequalities (11) correspond approximately to $\epsilon \gg 0.1$.

C. Thomas-Fermi Potential

Expanding the exponential in the integral

$$\int_0^{\gamma\varepsilon}\omega(u)\,e^{-i\lambda u} - 1)\,du$$

in a series and confining ourselves to the first four terms of the expansion, we obtain

$$f(r,\Delta) = \frac{1}{2\pi}\int_{-\infty}^{\infty}\exp\left[i\left(\alpha\lambda - rJ_1\lambda + \frac{1}{6}\lambda^3\gamma^2 J_3 r\right) - \frac{\lambda^2}{2}\gamma r J_2\right]d\lambda. \quad (22)$$

We have introduced in (22) the notation

$$\alpha = \Delta - r\left(\frac{d\varepsilon}{dr}\right)_e \qquad J_m = \frac{1}{\gamma^m}\int_0^{\gamma\varepsilon} u^m\omega(u)\,du \qquad (m = 1, 2, 3). \quad (22')$$

Carrying out in (22) transformations similar to those made above, we obtain

$$f(r,\Delta) = b_1^{-1/2}\chi(\lambda_1), \quad (23)$$

where

$$\chi(\lambda_1) = \frac{1}{\pi}\int_0^\infty e^{-x^2}\cos(\lambda_1 x + \delta x^3)\,dx, \quad (24)$$

$$\lambda_1 = \frac{\Delta - r[(d\varepsilon/dr)_e + J_1]}{b_1^{1/2}}, \quad b_1 = \frac{rJ_2\gamma}{2}, \quad \delta = \frac{\sqrt{2}}{3}\left(\frac{\gamma}{r}\right)^{1/2}Sk_\Delta, \quad Sk_\Delta = \frac{J_3}{J_2^{3/2}}. \quad (25)$$

Thus, $f(r, \Delta)$ can be expressed in terms of the universal function $\chi(\lambda_1)$ of the dimensionless variable λ_1. The most probable value of the energy loss is calculated from the formula

$$\Delta_0 = r\left[\left(\frac{d\varepsilon}{dr}\right)_e + J_1\right] + b_1^{1/2}\lambda_{1max}. \quad (26)$$

The moments J_m of the function $\omega(u)$ were calculated with a computer on the basis of the function $f(t^{1/2})$, and the values $J_1 = S_n$ and $J_2 = Sk_\Delta$ are listed in Table I for different values of ϵ. Figure 5 shows plots of $\chi(\lambda_1)$ calculated with a computer for four values of the parameter δ, and also plots of the integral probability

for the energy loss exceeding λ_1, i.e.,

$$\int_{\lambda_1}^{\infty}\chi(x)dx=\psi(\lambda_1) \tag{27}$$

for the same values of the parameter δ.

Let us determine the conditions for the applicability of the results. The expansion (22) is valid if $\lambda u_{max} \ll 1$, where λ is taken to mean the value playing the principal role in the integral (22), i.e., $\lambda \sim b_1^{-1/2}$. From this we obtain that the condition for the applicability of the expansion (22) is

$$\gamma\varepsilon^2/rJ_2 \ll 1. \tag{28}$$

The condition (28) corresponds approximately to $\epsilon \ll 0.1$. Recognizing that $\omega(u)$ is very small for values of u close to the maximum, the range of applicability of the function $\chi(\lambda_1)$ is larger than that given by condition (28). We note that if the asymmetry parameter Sk_Δ is equal to zero, then Eq. (24) leads to a Gaussian distribution of the fluctuations with an rms deviation $b_1^{1/2}$. This distribution can be used to determine the fluctuations in thick layers comparable with the total free path (see[5]). It should also be noted that in the intermediate region of values of ϵ, in which the results of subsections A and B are not valid, the most probable energy loss Δ_0 is close to $I = r(J_1 + K\epsilon^{1/2})$ (compare (20) with (26)).

2. CORRECTION FOR THE TRUE PATH LENGTH

In the calculations of Sec. 1 it was assumed that the paths of all the particles passing through a layer of matter r are identical and coincide with the layer of thickness. Actually, the ion paths ρ in the layer are different and in the general case are not equal to r.

We rewrite (3) in the form

$$\frac{\partial}{\partial\rho}f(\rho,\Delta)=\frac{1}{\gamma}\int_0^{\gamma\varepsilon}\omega(u)\,[f(\rho,\Delta-u)-f(\rho,\Delta)]\,du - \left(\frac{d\varepsilon}{dr}\right)_*\frac{\partial}{\partial\Delta}f(\rho,\Delta)+\left(1-\frac{r}{\rho}\right)\frac{\partial f(\rho,\Delta)}{\partial\rho}. \tag{29}$$

When $\rho = r$ Eq. (29) goes over into (3). It is assumed that $\Delta \ll \epsilon$ and r/ρ is close to unity, so that the correction connected with multiple scattering is small. Therefore, in the perturbation-theory approximation, we represent the sought function f as follows:

$$f=f_1+f_2, \tag{30}$$

where $f_2 \ll f_1$ and f_1 is the solution of Eq. (3). Substituting (30) in (29) we obtain an equation for the function f_2:

$$\frac{r}{\rho}\frac{\partial f_2}{\partial\rho}=\frac{1}{\gamma}\int_0^{\gamma\varepsilon}\omega(u)\,[f_2(\rho,\Delta-u)-f_2(\rho,\Delta)]\,du - \left(\frac{d\varepsilon}{dr}\right)_*\frac{\partial f_2}{\partial\Delta}+\left(1-\frac{r}{\rho}\right)\frac{\partial f_1}{\partial\rho}. \tag{31}$$

Expanding the integrand of (31) in a Taylor series and confining ourselves to the first two terms of the expansion, we obtain

$$\left(\frac{r}{\rho}+J_1\frac{\partial\rho}{\partial\Delta}+K\varepsilon^{1/2}\frac{\partial\rho}{\partial\Delta}\right)\frac{\partial f_2}{\partial\rho}=\left(1-\frac{r}{\rho}\right)\frac{\partial f_1}{\partial\rho} \tag{32}$$

The multiple-scattering effect is large at low ion energies, when the energy loss due to elastic collisions predominates. Taking this into account, we put K = 0. Further, inasmuch as ρ/r is quite close to unity, we replace the sum $\rho/r + 1$ by 2. Integrating (32) with allowance for these assumptions, we obtain for the case of a power-law potential

$$f_2=\frac{1}{2}\left(\frac{\rho}{r}-1\right)f_1-\frac{1}{2r}\int_0^{\rho}f_1\,d\rho. \tag{33}$$

The sought function f is equal to

$$f=\frac{1}{2}\left(\frac{\rho}{r}+1\right)f_1-\frac{1}{2r}\int_0^{\rho}f_1\,d\rho. \tag{34}$$

Let us calculate $f(\rho, \Delta)$, taking f_1 to be the function defined in (10′), i.e., $\varphi(\xi)$. In this case

$$\rho=\frac{1}{\lambda_2}\Delta,\quad \frac{\langle\rho(\Delta)\rangle}{r}\approx 1+\frac{1}{3}\mu\quad\left(\mu=\frac{A_2}{A_1}\text{ for }A_1>A_2\text{[1]}\right).$$

We find therefore that the correction connected with multiple scattering is small if $(\langle\Delta\rangle/\lambda_2 r - 1) \ll 1$. In particular, when $A_1 \gg A_2$ this condition is replaced by $\mu \ll 1$.

If the following condition is satisfied

$$\frac{(\lambda_2 r)^2}{4\gamma\Delta\varepsilon}\sim\frac{1}{4\gamma}\frac{\Delta}{\varepsilon}\ll 1, \tag{35}$$

then we can neglect the second term of (34). Representing ρ in the form

$$\rho(\Delta)=r+\frac{1}{\lambda_2}(\Delta-\langle\Delta\rangle)=r+\frac{1}{\lambda_2}(\Delta-\beta^2)\text{ for }\Delta>\beta^2, \tag{36}$$

we obtain ultimately

$$f=\left(1+\frac{\Delta-\beta^2}{2\lambda_2 r}\right)f_1. \tag{37}$$

The dashed curves in Fig. 2 are the distribution func-

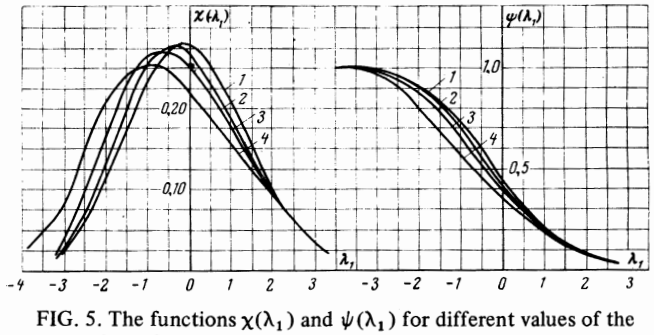

FIG. 5. The functions $\chi(\lambda_1)$ and $\psi(\lambda_1)$ for different values of the parameter δ: 1–δ = 0.1, 2–δ = 0.3, 3–δ = 0.5, 4–δ = 1.0.

Table I. Moments of the function $\omega(u)$ and the asymmetry parameter Sk_Δ

ε	J_1	J_2	Sk_Δ	ε	J_1	J_2	Sk_Δ
0,05	0.355	0.007	0.510	0.6	0.373	0.075	1.282
0.1	0.372	0.014	0.521	0,7	0.360	0.084	1.404
0.2	0.400	0.029	0.712	0,8	0.359	0.092	1.524
0,3	0.404	0.043	0.874	0,9	0.358	0.099	1.641
0.4	0.405	0.055	1.019	1.0	0.356	0.106	1.756
0,5	0.383	0.066	1.154				

Table II. Comparison of theoretical and experimental values

Ion	Target	Target thickness Å	Ion energy E, keV	ΔE, keV	Δ_0 experiment	Δ_0 theory	b	K_0	K_1	Δ_{01}	S_e/S_n	I	Reference
Li^7	Cu	140	11	3,25	0.325	0.28	0.012	0,58	0.88	—	1.67	0.24	[6]
			13	3.50	0.35	0.28	0.010	0.58	0.95	—	1.91	0.25	
			15	3.70	0.37	0.26	0.009	0.58	0.99	—	2.12	0,26	
			17	3.80	0.38	0.27	0.008	0.58	0.97	—	2.31	0,265	
Ne^{20}	C	106	67,2	2,70	0.19	0.244	0.007	0.11	0,09	0.21	1.10	0.39	[7]
Ar^{40}	C	335	200	26.0	0.56	0,62	0.019	0.10	0.10	0.62	1.0	0,67	[8]
Ge^{74}	C	235	400	9,5	0.06	0.23	0.012	0.10	0.07	0.21	0.60	0.24	[4]

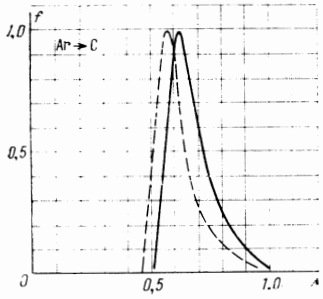

FIG. 6. Plots of the scatter of the energy loss of Ar^{40} ions in carbon (E = 200 keV); solid curve–theory, dashed–experiment.

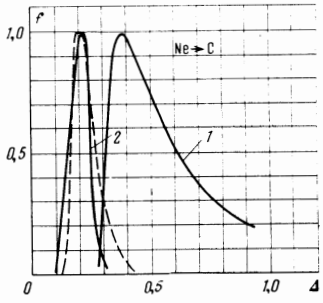

FIG. 7. Plots of the scatter of the energy loss of Ne^{20} ions in carbon (E = 67.2 keV); solid curve–theory ($1-\lambda_{3/2} = 0.25$; $2-\lambda_{3/2} = 0.216$), dashed–experiment.

tions of the energy loss with allowance for multiple scattering (we consider the case $\epsilon = 1$, $\gamma = 0.2$, $r = 0.3$, and $r/\langle\rho\rangle = 0.1$); the plot of the function f constructed with allowance for the second term of (34) is shown by a dash-dot line. From an analysis of the curves of Fig. 2 it follows that the correction to $\varphi(\xi)$, due to the multiple scattering, is small. This indicates that we can use the first approximation in r/ρ in the series expansion of the function.

3. COMPARISON WITH EXPERIMENT

Unfortunately, so far only few published papers give data on the energy loss of low-energy charged particles (with energy E smaller than several hundred keV) in thin layers of matter. This is due mainly to the difficulty of performing experiments of low-energy ions and thin absorbers. Table II and Figs. 6 and 7 show a comparison of the theoretical and experimental values.

Figures 6 and 7 show plots of the energy loss of Ar^{40} and Ne^{20} ions, respectively, in carbon. For the $Ne^{20} \rightarrow C$ case, the calculations are given for two values of $\lambda_{3/2}$, 0.25 and 0.216. Table II[3)] gives the values of the most probable energy loss for ions, plots of which are shown in the figures, and also for Li^7 ions in copper and Ge^{74} ions in carbon. From an analysis of the theoretical and experimental values it follows that Δ_0 depends little on the values of b (i.e., on λ_3) and depends strongly on $C^{3/2}$ (i.e., on $\lambda_{3/2}$). As seen from Fig. 7, the approximation of the scattering function $f(t^{1/2})$ for large values of ϵ by means of the function $f_{3/2}(t^{1/2})$ with $\lambda_{3/2} = 0.25$ leads to an appreciable difference between the theoretical and experimental data. This is connected with the fact that for large ϵ and for light ions the values of t correspond to the first part of the plot of the scattering function, where the approximating curve $f_{3/2}(t^{1/2})$ with $\lambda_{3/2} = 0.25$ lies above the curve calculated in accordance with the Thomas-Fermi potential. At a smaller value of $\lambda_{3/2}$, the agreement with experiment is much better. Both in the case of Ar^{40} and of Ne^{20} ions, the difference in Δ_0 between the theoretical and experimental values does not exceed 10%.

As was noted above, the formula of the LSS theory for inelastic slowing down is approximate, since it does not take into account the shell structure of the atom. This is due to the fact that the LSS theory is based on the Thomas-Fermi statistical model of the atom. We have obtained, on the basis of the independent-particle nuclear model as applied to the atom, a formula for the slowing-down ability $(d\epsilon/d\rho)_S$ with allowance for an oscillatory dependence on Z_1 and a nonmonotonic dependence on Z_2. This formula, which describes satisfactorily the experimental data and is valid for $Z_1 \gtrsim 10$, is of the form

$$10^{14} S_e \left(\frac{\text{eV-cm}^2}{\text{atom}} \right) = 2.92 \xi_e \frac{d^3}{H^2} \Phi(\beta) \frac{Z_1 Z_2}{(Z_1^{2/3} + Z_2^{2/3})^{3/2}} S_{e,\text{LSS}}, \quad (38)$$

where $\xi_e \approx Z_1^{1/6}$, d and H are constants that depend on Z_1 $\Phi(\beta)$ is a function of the parameter $\beta = 1 - 1/H$ and is expressed in terms of confluent hypergeometric functions.

Table II lists values of K calculated in accordance with formula (4) (K_0) and in accordance with formula (38) (K_1), and also the values of Δ_{01} calculated using K_1. In the case of Li^7 ions, formula (38) does not hold. Table II lists, for the Li^7-Cu pair, the values of K_1 which reconcile the theoretical and experimental data. The constancy of the values of K_1 ($\langle K_1 \rangle \approx 0.94$, the maximum deviation from $\langle K_1 \rangle$ is less than 7%) and the predominance of electronic deceleration over elastic deceleration suggests that $K_1 \approx 0.90$, which should be obtained when account is taken of shell effects, is correct for the Li^7-Cu pair.

In the case of the Ge^{74} ions, the form of the experimental profile of the energy-loss-scatter curve coin-

[3)] The conditions (21) are satisfied for all the cases under consideration.

cides with the theoretical one, but the absolute values of Δ_0 differ significantly. For Ge^{74} ions, the correction to the value of K_0 is quite large, but when account is taken of this correction, the energy loss in elastic collisions only (0.063) exceeds the experimental value. Such a difference in Δ_0 may be connected, for example, with the fact that the carbon density assumed in the calculation does not agree with the carbon density used in the experiment.

Thus, the relations obtained in the present paper give the correct form of the energy-loss-scatter curve, and if the constant $\lambda_{3/2}$ is correctly chosen an account is taken of the shell correction in K, the relations lead to satisfactory agreement with the known experimental data.

[1] S. V. Starodubtsev and A. M. Romanov, Prokhozhdenie zaryazhennykh chastits cherez veshchestvo (Passage of Charged Particles through Matter), AN UzSSR, Tashkent, 1962.

[2] J. Lindhard, M. Scharff and H. Schiott, Kgl. Dan. Vid. Selsk. Mat. Fys. Medd. 33, No. 14 (1963).

[3] J. Lindhard, V. Nielsen and M. Scharff, Kgl. Dan. Vid. Selsk. Mat. Fys. Medd. 36, No. 10 (1968).

[4] P. Hvelplund and B. Fastrup, Phys. Rev. 165, 408 (1968).

[5] I. Pomaranchuk, Zh. Eksp. Teor. Fiz. 18, 759 (1948).

[6] E. M. Zarutskiĭ, Fiz. Tverd. Tela 9, 1896 (1967) [Sov. Phys.-Solid State 9, 1495 (1968)].

[7] J. Ormrod and H. Duckworth, Canad. J. Phys. 41, 1424 (1963).

[8] B. Fastrup, P. Hvelplund and C. Saufter, Kgl. Dan. Vid. Selsk. Mat. Fys. Medd. 35, No. 10 (1966).

Translated by J. G. Adashko